Universiteit Leiden
The Netherlands

Accurate quantification of T cells in copy number stable and unstable DNA samples using multiplex digital PCR
Nell, R.J.; Zoutman, W.H.; Calbet-Llopart, N.; Garcia, A.P.; Menger, N.V.; Versluis, M.; ... ; Velden, P.A. van der

Accurate Quantification of T Cells in Copy Number Stable and Unstable DNA Samples Using Multiplex Digital PCR

Check for updates

Rogier J. Nell,* Willem H. Zoutman,[†] Neus Calbet-Llopart,[‡] Adriana P. Garcia,[§] Nino V. Menger,* Mieke Versluis,* Susana Puig,[‡] Nelleke A. Gruis,[†] and Pieter A. van der Velden*

From the Departments of Ophthalmology and Dermatology,[†] Leiden University Medical Center, Leiden, the Netherlands; the Department of Dermatology,[‡] Hospital Clínic de Barcelona, Institut d'Investigacions Biomèdiques August Pi Sunyer (IDIBAPS), University of Barcelona, Centro Investigación Biomédica en Red de Enfermedades Raras, Instituto de Salud Carlos III, Barcelona, Spain; and the Department of Pathology,[§] Hospital Clínic de Barcelona, Barcelona, Spain*

An accurate T-cell quantification is prognostically and therapeutically relevant in various malignancies. We previously developed a digital PCR—based approach offering a precise T-cell enumeration in small amounts of DNA. However, it may be challenging to apply this method in malignant specimens, as genetic instability can disturb the underlying mathematical model. For example, approximately 24% of the tumors from The Cancer Genome Atlas pan-cancer data set carried a copy number alteration affecting the *TRB* gene T-cell marker, which would cause an underestimation or overestimation of the T-cell fraction. In this study, we introduce a multiplex digital PCR experimental setup to quantify T cells in copy number unstable DNA samples. By implementing a so-called regional corrector, genetic alterations involving the T-cell marker locus can be recognized and corrected for. This novel setup is evaluated mathematically *in silico* and validated *in vitro* by measuring T-cell presence in various samples with a known T-cell fraction. The utility of the approach is further demonstrated in copy number altered cutaneous melanomas. Our novel multiplex setup provides a simple, but accurate, DNA-based T-cell quantification in both copy number stable and unstable specimens. This approach has potential clinical and diagnostic applications, as it does not depend on availability of T-cell epitopes, has low requirements for sample quantity and quality, and can be performed in a relatively easy experiment. *(J Mol Diagn 2022, 24: 88—100; https://doi.org/10.1016/j.jmoldx.2021.10.007)*

T cells form a crucial part of the adaptive immune system, the most specified form of our body's defense system. T cells are able to recognize an almost infinite diversity of pathogenic antigens by their T-cell receptor, a unique molecule that is highly variable among different T cells. This variability is the result of several genetic mechanisms occurring during early maturation of these cells in the thymus.[1,2] One of these involves the rearrangement of the germline T-cell receptor genes (*TRD*, *TRG*, *TRB*, and *TRA*) into a unique T-cell receptor blueprint. Selection procedures ensure that only T cells with functional recombinations are released into the periphery.[3] Consequently, all T cells found in any organ or tissue have

genetically altered T-cell receptor genes, whereas all other cell types carry these genes in the unaltered germline configuration.

On the basis of these genetic dissimilarities, we previously identified and validated two generic T-cell DNA markers: ΔB (located within the *TRB* gene) and ΔD (located within the *TRD* gene).[4] In contrast to a copy number invariant genomic reference, which is present on both alleles in any cell, both T-cell markers are biallelically absent in nearly all T cells. Therefore, the relative absence of a T-cell marker compared with the reference equals the fraction of T cells. By using duplex digital PCR, an absolute quantification of both targets could be established, thereby offering a DNA-based method to accurately quantify T cells.[4,5]

This experimental rationale, referred to as the classic model, allows us to measure T-cell presence under the assumption of genomic stability of the target and reference loci. This requirement is typically met when a DNA sample of nonmalignant origin is analyzed; benign samples, in general, do not present with copy number alterations (CNAs). However, in malignant samples, admixed copy number unstable cancer cells may complicate DNA-based T-cell quantifications, given that around 90% of the solid tumors harbor somatic CNAs.[6]

Still, it may be particularly advantageous to perform a T-cell quantification in malignant samples, as the presence of tumor-infiltrating T cells is prognostically and therapeutically relevant in various types of cancer.[7,8] Moreover, as tumor material (eg, small biopsies) is frequently scarce or of limited quality, golden standard methods like flow cytometry and immunohistochemistry may be unfeasible, whereas DNA-based analyses remain possible.

Practically, copy number instability may result in the loss or gain of the target (ie, the T-cell marker ΔB or ΔD) and/or reference locus. As a consequence, determined T-cell fractions will be underestimated or overestimated. Reference instability can be corrected by using another reference: in principle, any disomic locus of the genome may suffice.[5] The selection of a putative stable reference is often guided by knowledge about copy number stability in the tumor type of interest or a sample-specific analysis. In contrast, CNAs affecting the T-cell markers, which have strict genomic locations within the *TRB* and *TRD* genes, cannot be resolved in a similar way and will have detrimental consequences on the calculation of the T-cell fraction. As the ΔB and ΔD markers are located on different chromosomes (7q and 14q, respectively), switching to the other marker may overcome this problem, but then the copy number state of both loci should be known. Moreover, when a sample presents with CNAs on both chromosomes, it is no longer possible to accurately determine the T-cell presence using the classic model.

In this study, we introduce an extension (referred to as the adjusted model) of our original experimental rationale, allowing the recognition and automatic correction of CNAs affecting the T-cell marker region. This adjusted model is evaluated *in silico* and validated *in vitro* using multiplex digital PCR. Moreover, the utility of the proposed experimental setup is demonstrated by measuring T-cell presence in DNA samples from copy number altered cutaneous melanomas.

Materials and Methods

Pan-Cancer Analysis

To investigate the presence of CNAs affecting the ΔB and ΔD T-cell marker regions in cancer (Figure 1), The Cancer Genome Atlas pan-cancer data set was studied using the copy number and merged sample quality annotations data obtained via The Pan-Cancer Atlas (PanCanAtlas, *https://gdc.cancer.gov/about-data/publications/pancanatlas*, last accessed May 31, 2021).[6,9] The lymphoid neoplasm diffuse large B-cell lymphoma and acute myeloid leukemia data sets were excluded as in these tumours lymophocytes form the malignant cell population and/or illegitimate rearrangements of the T-cell receptor genes have been reported.[10,11] For each tumor-derived sample, the segment mean copy number values for the *TRB* and *TRD* gene loci were assessed by using a noise cutoff threshold value of 0.3: values smaller than −0.3 were categorized as loss, and values larger than 0.3 were categorized as gain. For each tumor type, the frequency of cases with a loss, gain, or no CNA was calculated, and pan-cancer statistics were determined by taking the mean of the frequencies per tumor type. Affected cases were further studied by determining the copy number state of the entire chromosomes. The complete analysis was performed using R version 4.0.3, RStudio version 1.4.1103, and R package *data.table* version 1.13.6. All custom scripts are available in GitHub (*https://github.com/rjnell/t-cell-quantification*, last accessed October 18, 2021).

Classic Model

In the classic model, two DNA markers are quantified to determine the T-cell fraction: T-cell marker ΔB (or ΔD) and a copy-number stable, independent genomic reference REF (Figure 2A). The quantifications obtained by digital PCR are indicated by [ΔB] and [REF], respectively, and are usually measured in copies/μL.
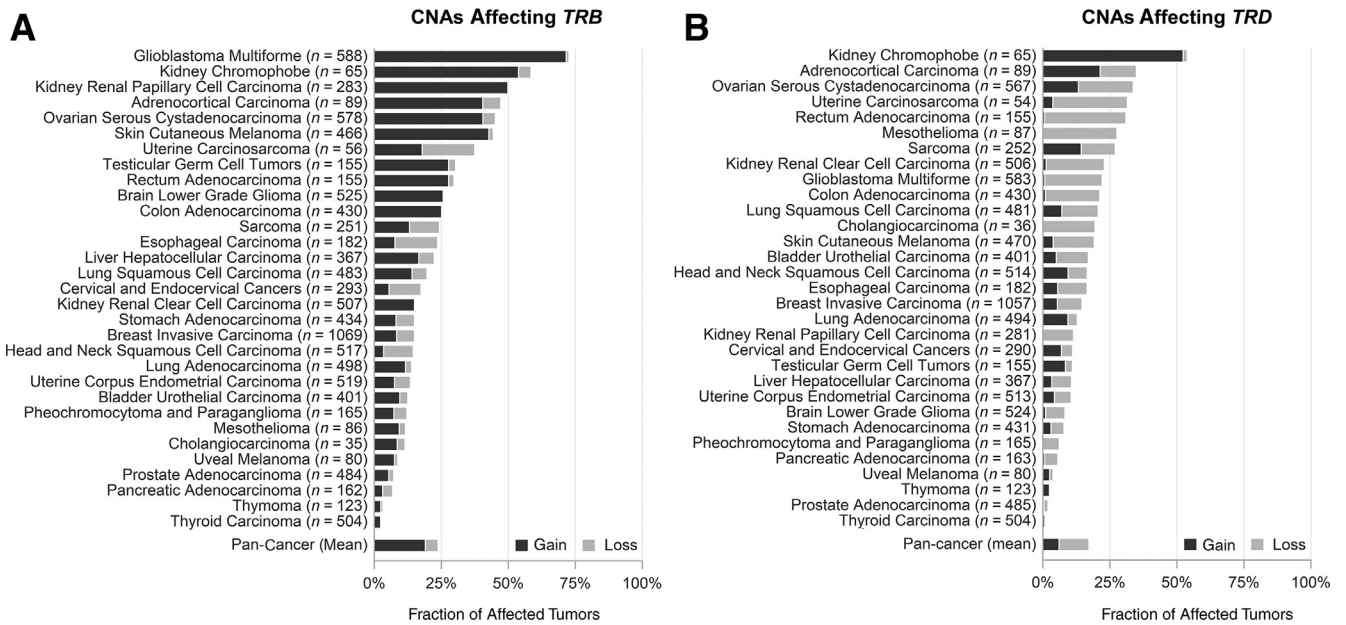
ΔB (or ΔD) is present on 0 alleles derived from T cells, and present on two alleles derived from all other cells:
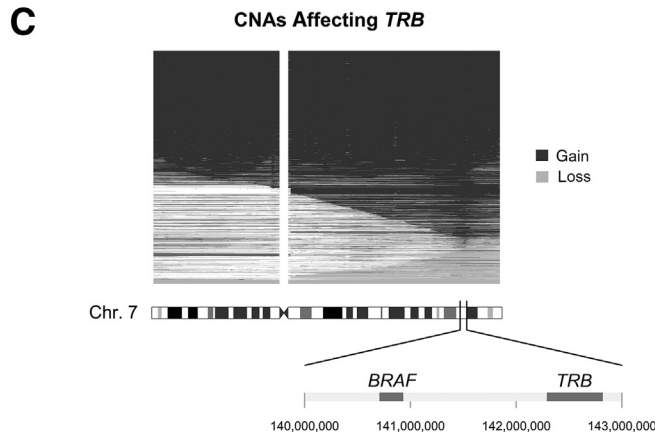
$$[\Delta B] = 0 \cdot TCF + 2 \cdot (1 - TCF) \tag{1}$$

$$= 2 \cdot (1 - TCF) \tag{2}$$

REF is present on two alleles derived from T cells, and present on two alleles derived from all other cells:

$$[REF] = 2 \cdot TCF + 2 \cdot (1 - TCF) \tag{3}$$

A CNAs Affecting *TRB*

B CNAs Affecting *TRD*

C CNAs Affecting *TRB*

Figure 1 Pan-cancer analysis of copy number alterations (CNAs) involving the T-cell marker loci. Chromosomal gains and losses are studied in 10,550 tumor samples across 31 cancer types. **A:** On average, approximately 24% of the cases presented with a CNA of the *TRB* gene, in which the ΔB marker is located. **B:** CNAs of the *TRD* gene, in which the ΔD marker is located, were found in on average approximately 17% of the cases. **C:** The gains and losses of the *TRB* gene originate from complete chromosome (Chr.) 7 CNAs in about half of the affected cases. More focal alterations frequently involve both *TRB* and *BRAF*, an established oncogene located in close proximity of the *TRB* gene.

$$= 2 \tag{4}$$

The ratio $\frac{[\Delta B]}{[REF]}$ can then be rewritten as follows:

$$\frac{[\Delta B]}{[REF]} = \frac{2 \cdot (1 - TCF)}{2} \tag{5}$$

$$= 1 - TCF \tag{6}$$

which results in the formula to calculate the T-cell fraction:

$$TCF = 1 - \frac{[\Delta B]}{[REF]} \tag{7}$$

This ratio and its corresponding CI can be calculated as described earlier.[12]

Adjusted Model

In the adjusted model, three DNA markers are quantified: T-cell marker ΔB (or ΔD), regional corrector (RC) RC$_{\Delta B}$ (or RC$_{\Delta D}$), and a copy-number stable, independent genomic reference REF (Figure 2B). The quantifications using digital PCR are indicated by [ΔB], [RC$_{\Delta B}$], and [REF], respectively.

ΔB is present on 0 alleles derived from T cells, and present on 2 + A alleles derived from other, possibly malignant cells:

$$[\Delta B] = 0 \cdot TCF + (2 + A) \cdot (1 - TCF) \tag{8}$$
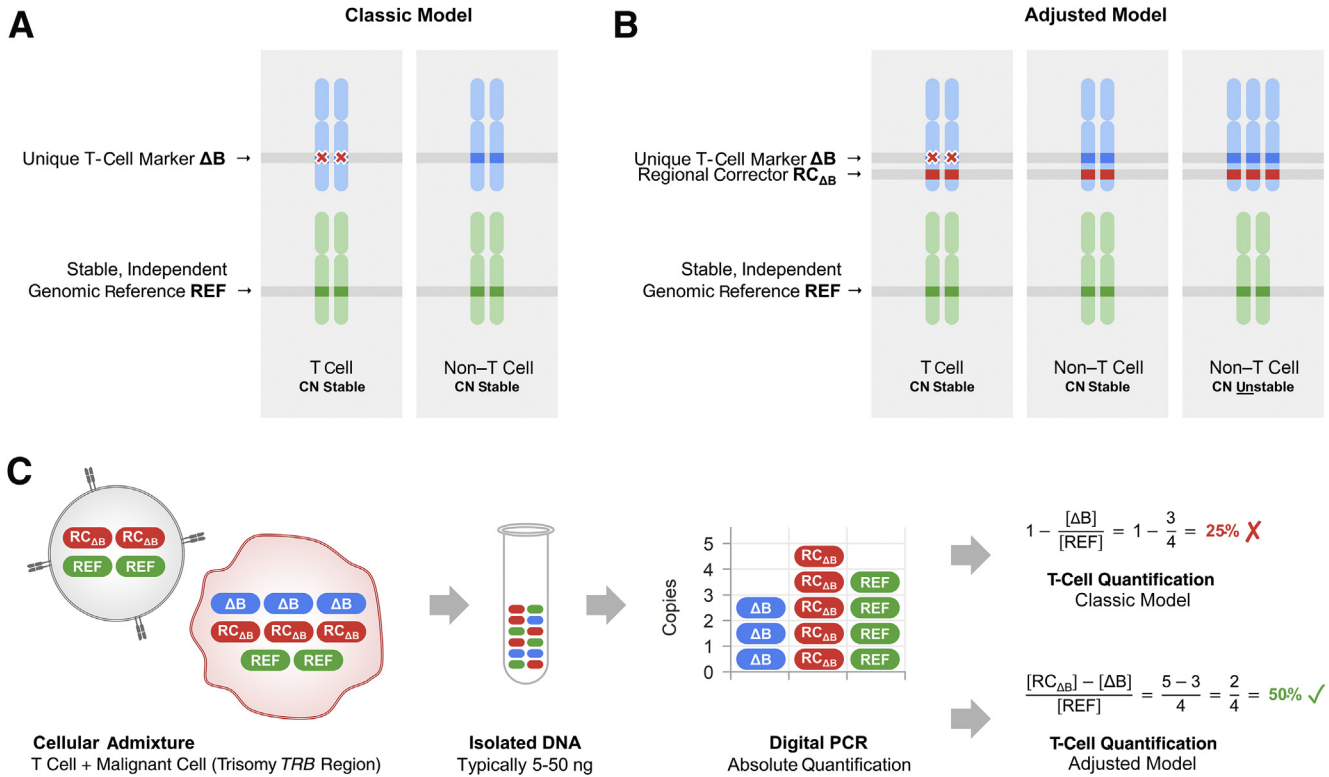
$$= (2 + A) \cdot (1 - TCF) \tag{9}$$

RC$_{\Delta B}$ is present on 2 alleles derived from T cells and present on 2 + A alleles derived from other, possibly malignant cells:

$$[RC_{\Delta B}] = 2 \cdot TCF + (2 + A) \cdot (1 - TCF) \tag{10}$$

Figure 2 Models and workflow to obtain T-cell quantification using digital PCR. **A:** T-cell quantification using T-cell marker ΔB and reference REF, according to the classic model. T cells have lost ΔB biallelically, whereas other cells carry two copies of ΔB. Independent and stable genomic reference REF is present on two alleles in all cells. **B:** T-cell quantification using T-cell marker ΔB, regional corrector $RC_{\Delta B}$, and reference REF, according to the adjusted model. The classic model from **A** is extended with regional corrector $RC_{\Delta B}$. This is a target located at the same chromosomal arm and in close proximity to ΔB. However, $RC_{\Delta B}$ is not affected by T-cell receptor rearrangements during the development of T cells, so all copy number (CN) stable cells have two copies of $RC_{\Delta B}$. However, when a CNA in a non—T cell involves the ΔB T-cell marker region, this equally affects ΔB and $RC_{\Delta B}$. **C:** Workflow example of obtaining the T-cell quantification in a cellular admixture of one T cell and one copy number unstable non—T cell with a gain of the T-cell marker region at chromosome 7. Typically, 5 to 50 ng of isolated DNA is analyzed for T-cell marker ΔB, regional corrector $RC_{\Delta B}$, and reference REF using digital PCR. Determined abundances of the targets are used to calculate the T-cell fraction, according to the classic and adjusted model. Following the classic model, an incorrect T-cell fraction of 25% is calculated. According to the adjusted model, the CNA involving the T-cell marker region is recognized and adjusted for; a correct T-cell fraction of 50% is calculated.

$$[RC_{\Delta B}] - [\Delta B] = 2 \cdot TCF + (2 + A) \cdot (1 - TCF) - (2 + A) \cdot (1 - TCF) \tag{11}$$

$$= 2 \cdot TCF \tag{12}$$

REF is present on two alleles derived from T cells, and present on two alleles derived from all other cells:

$$[REF] = 2 \cdot TCF + 2 \cdot (1 - TCF) \tag{13}$$

$$= 2 \tag{14}$$

The ratio $\frac{[RC_{\Delta B}] - [\Delta B]}{[REF]}$ can then be rewritten as follows:

$$\frac{[RC_{\Delta B}] - [\Delta B]}{[REF]} = \frac{2 \cdot TCF}{2} \tag{15}$$

$$= TCF \tag{16}$$

which results in the formula to calculate the T-cell fraction:

$$TCF = \frac{[RC_{\Delta B}] - [\Delta B]}{[REF]} \tag{17}$$

As described by Dube et al,[12] the concentration of a given target (eg, [ΔB]) can be calculated from the observed fraction of digital PCR partitions being positive for this target ($p_{\Delta B+}$) as follows:

$$[\Delta B] = \frac{-\log(1 - p_{\Delta B+})}{V} \tag{18}$$

$$= \frac{-\log(p_{\Delta B-})}{V} \tag{19}$$

where $p_{\Delta B+}$ denotes the observed fraction of partitions being positive for target ΔB and V the volume of one partition (ie, a droplet).

The numerator of the ratio in equation 17 can be rewritten as follows:

$$[RC_{\Delta B}] - [\Delta B] = \frac{-\log(p_{RC_{\Delta B^-}})}{V} - \frac{-\log(p_{\Delta B^-})}{V} \quad (20)$$

$$= \frac{-\left(\log(p_{RC_{\Delta B^-}}) - \log(p_{\Delta B^-})\right)}{V} \quad (21)$$

$$= -\frac{\log\left(\frac{p_{RC_{\Delta B^-}}}{p_{\Delta B^-}}\right)}{V} \quad (22)$$

where V is a constant value, and $\log\left(\frac{p_{RC_{\Delta B^-}}}{p_{\Delta B^-}}\right)$ a log-ratio of two binomial distributions, which is approximately normally distributed,[13] with variance:

$$\mathrm{Var} = \frac{p_{RC_{\Delta B^-}}^{-1} - 1}{n_{RC_{\Delta B}}} + \frac{p_{\Delta B^-}^{-1} - 1}{n_{\Delta B}} \quad (23)$$

where $n_{RC_{\Delta B}}$ and $n_{\Delta B}$ denote the total number of droplets being analyzed in the experiments determining $[RC_{\Delta B}]$ and $[\Delta B]$, respectively. These numbers are equal to each other (n) when both targets are measured simultaneously in one experiment:

$$\mathrm{Var} = \frac{p_{RC_{\Delta B^-}}^{-1} + p_{\Delta B^-}^{-1} - 2}{n}$$

Now, similar to the approach of Dube et al,[12] the numerator of equation 17 can be calculated with accompanying CI, which is used in the construction of the final ratio CI of equation 17, the T-cell fraction according to the adjusted model, itself.

Note that when $[RC_{\Delta B}] = [REF]$ (ie, when no CNA is affecting the $RC_{\Delta B}$ region), the adjusted model (equation 17) resolves into the classical model (equation 7):

$$\frac{[RC_{\Delta B}] - [\Delta B]}{[REF]} = \frac{[REF] - [\Delta B]}{[REF]} \quad (25)$$

$$= 1 - \frac{[\Delta B]}{[REF]} \quad (26)$$

In Silico Simulations

The basis of the *in silico* simulations is described in Supplemental Appendix S1. For the analysis, R version 4.0.3, RStudio version 1.4.1103, and R packages *rmarkdown* version 2.7 and *digitalPCRsimulations* version 1.1.0, available via GitHub (*https://github.com/rjnell/digitalPCRsimulations*, last accessed October 18, 2021), were used.

Collection, DNA Isolation, and Flow Cytometry of Reference Samples

Healthy peripheral blood mononuclear cell (PBMC) samples with determined CD3+ T-cell fractions were available

from our previous study.[4] In short, peripheral heparinized blood was drawn from healthy donors and PBMCs were isolated by Ficoll density gradient centrifugation. Flow cytometry was performed using CD3-allophycocyanin conjugated monoclonal antibodies (BD Biosciences, San Jose, CA; catalog number 345767), a FACSCalibur flow cytometer (BD Biosciences), and FlowJo software version 7.2.5 (FlowJo, Ashland, OR). Uveal melanoma cell line Mel-202[14] was available in the Department of Ophthalmology, Leiden University Medical Center, Leiden, the Netherlands. DNA was isolated using the QIAmp DNA Mini Kit, according to the protocol supplied by the manufacturer (Qiagen, Hilden, Germany).

Collection, DNA Isolation, and Immunohistochemistry of Cutaneous Melanomas

Biopsies from two primary tumors and one cutaneous metastasis from three cutaneous melanoma patients were collected from the Department of Dermatology, Hospital Clínic of Barcelona, Barcelona, Spain. All patients gave their written informed consent. DNA was isolated from fresh-frozen tumor specimens using the TissueLyser LT (Qiagen) and the QIAmp DNA Mini Kit (Qiagen), following the manufacturer's recommendations. Paraffin blocks were available of the same samples, from which tissue sections (3 μm thick) were cut and transferred to glass slides for staining by immunohistochemistry. The staining was performed using rabbit polyclonal CD3 antibody (Cell Marque Corp., Rocklin, CA) on the Ventana Benchmark platform (Ventana Medical Systems, Oro Valley, AZ), as recommended by the manufacturer. Tumor infiltrating lymphocytes were quantified by counting CD3+ immunopositive cells. For each sample, five representative tumor areas were evaluated with a 400-fold magnification (high-power fields). Images were captured with an Olympus SC50 digital camera (Olympus, Tokyo, Japan), and enumeration of cells was performed using the cellSens Standard software version 3.1 (Olympus).

Digital PCR

Digital PCR experiments were performed using the QX200 Droplet Digital PCR System (Bio-Rad Laboratories, Hercules, CA), following the general experimental guidelines, as described earlier.[5] In short, 20 ng of DNA was analyzed in a 22 μL experiment, using 11 μL ddPCR Supermix for Probes (no dUTP; Bio-Rad Laboratories) and primers and probes in a final concentration (optimized for multiplexing) of 1150 and 320 nmol/L, respectively, for the ΔB assay (Sigma-Aldrich, Gillingham, UK), and in an amount of 1.0 μL for premixed assay $RC_{\Delta B}$ targeting *TRBC2* (Sigma-Aldrich) and 1.4 μL for premixed reference assay targeting *TTC5* (Bio-Rad Laboratories). Two units of restriction enzyme HaeIII (New England Biolabs, Ipswich, MA) were added to each reaction mixture to enhance the accessibility

of all targets and prevent unwanted linkage between the T-cell marker and the RC. Minimum Information for Publication of Quantitative PCR Experiments (MIQE) context sequences and supplier information of all assays are provided in Table 1.

PCR mixtures were partitioned into 20,000 droplets using the AutoDG System (Bio-Rad Laboratories). Subsequent PCR was performed in a T100 Thermal Cycler (Bio-Rad Laboratories) using the following protocol: 10 minutes at 95°C; 30 seconds at 94°C and 1 minute at 60°C for 40 cycles; 10 minutes at 98°C; and cooling at 12°C until droplet reading. Ramp rate was set to 2°C/second in all steps, and the lid temperature was set to 105°C. Reading of the droplets was performed using a QX200 Droplet Reader (Bio-Rad Laboratories).

Raw digital PCR results were acquired using *QuantaSoft* version 1.7.4 (Bio-Rad Laboratories) and imported in online digital PCR management and analysis application *Roodcom WebAnalysis* version 1.9.4 (Roodcom, Voorschoten, the Netherlands, license required for use).

Results

Pan-Cancer Analysis of Copy Number Alterations Affecting the T-Cell Marker Loci

To investigate the frequency and origin of CNAs affecting the ΔB and ΔD T-cell marker regions in cancer, the copy number profiles of 10,550 cases spanning 31 tumor types from The Cancer Genome Atlas pan-cancer data set were analyzed.[6,9] On average, approximately 24% of the tumors carried a CNA affecting the *TRB* gene (ΔB locus) and approximately 17% affecting the *TRD* gene (ΔD locus), but large differences were observed between cancer types (Figure 1, A and B). Further evaluation of the affected cases showed that these CNAs typically encompassed much larger genomic regions than the T-cell marker locus only. For example, ΔB gains originated from complete chromosome 7 alterations in about half of the affected cases. The more focal CNAs typically co-occurred with a gain of *BRAF*, an established and frequently amplified oncogene located 1.35 million bp centromeric from the *TRB* gene (Figure 1C).[15,16]

T-Cell Quantification in Copy Number Stable and Unstable Conditions

The original classic model to quantify T cells is summarized in Figure 2A.[4] The biallelic absence of the T-cell marker is measured against a stable and independent genomic reference, all under copy number invariant conditions. However, in genetically unstable samples, a CNA involving the T-cell marker region can distort this classic model: a gain or loss of T-cell marker DNA may be unjustly attributed to the absence or presence of T cells. Such CNA can be detected and normalized in the adjusted model by incorporation of an extra target: an RC (Figure 2B). This target is located in close proximity of the T-cell marker but is not affected by T-cell receptor rearrangements during T-cell development. When CNAs in non−T cells comprise the entire T-cell marker region, the RC will be involved likewise, enabling a mathematical correction of the disrupted T-cell quantification. An illustration of the complete analysis workflow following both models is presented in Figure 2C. The mathematical rationale is described in *Materials and Methods*.

In Silico Evaluation of Classic and Adjusted Model

To assess the performance and mathematical validity of both the classic and adjusted model, an *in silico* simulation of the experimental setups was designed (Supplemental Appendix S1). Hereby, many virtual digital PCR experiments could be performed under specified conditions, allowing for an extensive evaluation of the theoretical accuracy and precision of the obtained results.

For the *in silico* experiments, first a 50% T-cell fraction in 20 ng copy number stable genomic input DNA was simulated (Figure 3A). In both the classic and adjusted model, the point estimate had a mean around the true T-cell fraction of 50%, indicating that an accurate T-cell quantification was obtained. The calculated 95% CIs contained this true T-cell

Table 1   Sequence and Supplier Information of Digital PCR Assays

ΔB	Forward primer: 5′−GCCATGCACTTTCCCTTTCG−3′
	Reverse primer: 5′−ACAGAGTCCATCCACAGGG−3′
	Probe (FAM or HEX labeled): 5′−TGGACCCTCACAGAGGGAGCA−3′
TRBC2	Assay (Sigma-Aldrich, FAM labeled, premixed, 74 nucleotides)
	Context sequence [chromosome 7:142802468−142802593 (GRCh38)]:
	CCCCTGAAACCCTGAAAATGTTCTCTCTTCCACAGGTCAAGAGAAAGGAT
	TCCAGAGGCTAGCTCCAAAACCATCCCAGGTCATTCTTCATCCTCACCCA
	GGATTCTCCTGTACCTGCTCCCAATC
TTC5	Assay (dHsaCP2506733, Bio-Rad, HEX labeled, premixed, 59 nucleotides)
	Context sequence [chromosome 14:20289639−20289761 (GRCh38)]:
	TGGTCGCGATGCCACTGTGGCAACAGCCTGGCTGCTGGATCCCTGAGGC
	TTCCCATTCACCACTAGCAGGAGGGGCGTCTCCACTCGAACACTGGAAAA
	GGAATAGTCCTAGAAAAGACAGAC

FAM, 6-carboxyfluorescein; HEX, hexachloro-fluorescein.

fraction in 95.1% (classic model) and 95.0% (adjusted model) of the experiments. As these values are close to the intended 95%, they demonstrate the mathematical correctness of both models under the given copy number neutral conditions. Notably, the SD around the mean and absolute width of the CIs were larger in the adjusted model.

Next, a 50% T-cell fraction in 20 ng copy number unstable genomic input DNA was simulated. In the 50% non−T cells, a clonal trisomy of the T-cell marker region was simulated, reducing the total loss of the T-cell marker to 25% in the complete sample (similar to the situation in Figure 2C). This 25% was observed as the point estimate mean of the classic model (Figure 3B). However, this value does not reflect the correct T-cell fraction and shows the error of the classic model under such copy number unstable condition. Moreover, none of the calculated 95% CIs contained the true T-cell fraction. In the adjusted model, the point estimate had a mean around the true T-cell fraction of 50%, and the calculated 95% CIs contained this true T-cell

fraction in 95.2% of the experiments. Thus, the adjusted model was able to correctly quantify the T-cell presence under these copy number unstable conditions, whereas the classic model failed to determine the correct T-cell fraction.

In Vitro Validation of the Adjusted Model Using Multiplex Digital PCR

To validate the wet-laboratory performance of the adjusted model, an RC digital PCR assay $RC_{\Delta B}$ was designed, allowing the recognition and normalization of CNAs affecting the ΔB T-cell marker region within the *TRB* gene. This assay targets *TRBC2*, which is the second constant domain and last downstream gene segment of *TRB* (Figure 4A). Because *TRBC2* is not deleted during variable, diversity and joining (VDJ) rearrangements, it becomes the closest (and thus most generic) genomic locus that can be exploited as RC for the ΔB.[2]
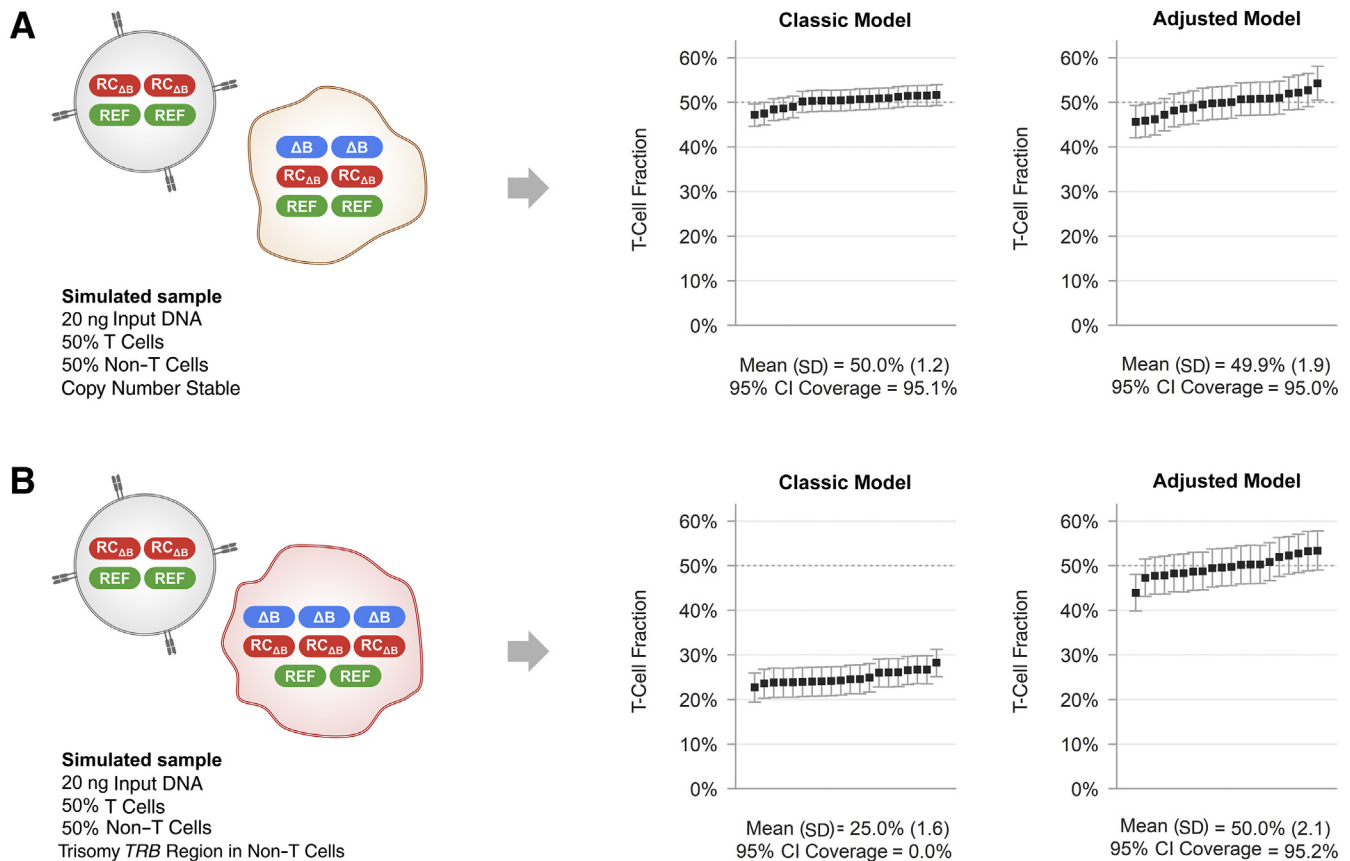
Figure 3 *In silico* evaluation of classic and adjusted model. The results of the first 20 simulated experiments per situation and model are sorted and plotted; the statistics of all simulations are presented below the plots. **A:** A total of 10,000 simulations of a 50% T-cell fraction in 20 ng copy number stable genomic input DNA. In both the classic and adjusted model, the point estimate has a mean around the true T-cell fraction of 50%. The calculated 95% CIs contain this true T-cell fraction in 95.1% (classic model) and 95.0% (adjusted model) of the experiments. However, the SD around the mean and absolute width of the CIs is larger in the adjusted model. **B:** A total of 10,000 simulations of a 50% T-cell fraction in 20 ng copy number unstable genomic input DNA. The 50% non−T cells present with a clonal trisomy of the T-cell marker region, reducing the total loss of the T-cell marker to 25% in the complete sample (similar to the situation in Figure 2C). This 25% is the point estimate mean of the classic model, but does not reflect the correct T-cell fraction. Moreover, none of the calculated 95% CIs contains the true T-cell fraction. In the adjusted model, the point estimate has a mean around the true T-cell fraction of 50%, and the calculated 95% CIs contain this true fraction in 95.2% of the experiments.

A *TRB* Gene Complex (7q34)
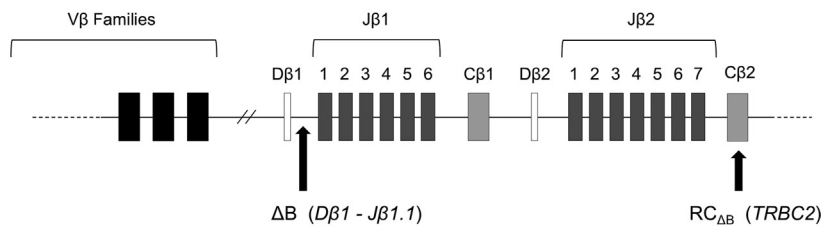
B
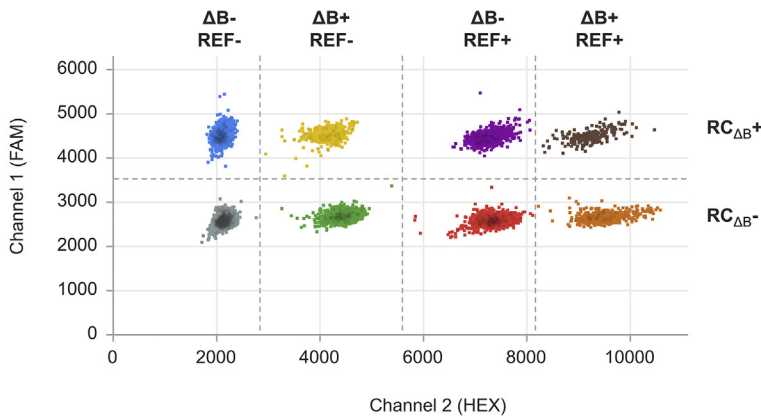
C
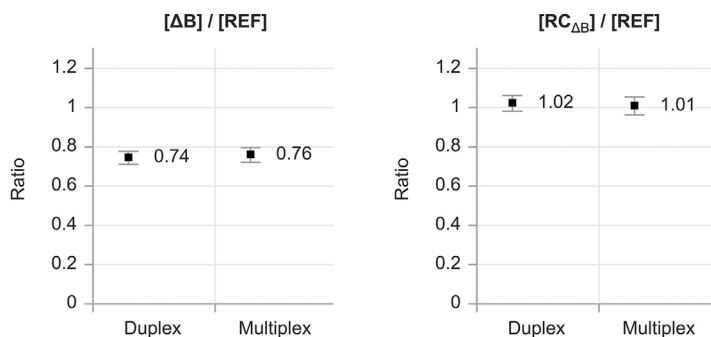
Figure 4   Determination of T-cell quantification, according to classic and adjusted model by multiplex digital PCR. **A:** Genomic position of the ΔB T-cell marker and its regional corrector $RC_{\Delta B}$ (targeting the *TRBC2* gene segment) on chromosome 7q34. Note that the copy-number invariant and independent genomic reference REF targets *TTC5*, which is located on chromosome 14q11.2. **B:** Two-dimensional plot of 1×2 multiplex digital PCR analyzing $RC_{\Delta B}$ on channel 1 (FAM: 6-carboxyfluorescein) and ΔB (assay with lowest fluorescence) and REF (assay with highest fluorescence) on channel 2 (HEX: hexachloro-fluorescein), leading to $2^3 = 8$ distinct clusters. **C:** Comparison of the concentration ratios, $[\Delta B]/[REF]$ and $[RC_{\Delta B}]/[REF]$, obtained by separate experiments with conventional duplex configuration, and the combined multiplex setup from **B**, showing similar results.

Previously, digital PCR experiments following the classic model were performed in a duplex configuration: the T-cell marker and reference were measured concurrently on two different channels.[4,5,17,18] The extension within the adjusted model, however, requires the measurement of one extra target (ie, the RC) in the sample of interest. Although this measurement may be performed in another duplex experiment (normalized to the same stable reference) and integrated into the calculation with the T-cell marker afterward, a multiplex analysis would be a more efficient solution. This setup can be performed with the same amount of DNA as in a traditional duplex experiment, but gives more information as the additional target is analyzed within the same well.[19,20]

The two-dimensional plot of such a multiplex digital PCR experiment is shown and annotated in Figure 4B. Herein, the

regional corrector $RC_{\Delta B}$ on channel 1 is analyzed simultaneously with T-cell marker ΔB (lowest fluorescence) and stable genomic reference REF (highest fluorescence) on channel 2. As droplets may or may not contain each of the three targets, $2^3 = 8$ different clusters can appear in a two-dimensional perspective. In such experiment, all three targets can be measured simultaneously, and the T-cell fraction can be calculated following the adjusted model. Notably, as ΔB and REF are both being determined with this multiplex, the T-cell fraction according to the classic model can also be calculated.

To validate this multiplex setup, a healthy PBMC DNA sample was analyzed, and the target concentration ratios were compared with those obtained from two separate duplex experiments (Figure 4C). Similar ratios were observed with both setups, but the two duplex experiments

required two times the amount of input DNA and experimental reagents compared with the single multiplex experiment. This demonstrates that a multiplex approach is equally valid, but more efficient, than the traditional duplex setups.

To confirm the *in silico* results regarding the adjusted model with *in vitro* experiments, the multiplex setup was applied in six healthy, copy number–stable PBMC samples for which flow cytometry–based T-cell quantifications were available (Figure 5A). Following both the classic and adjusted model, accurate T-cell fractions were obtained when compared with the fractions measured by flow cytometry. However, the observed variability (visualized by the 95% prediction interval) and 95% CIs of the measurements were larger using the adjusted model.

Second, our approach was validated in samples in which DNA from a healthy PBMC (containing approximately 60% T cells) was mixed with DNA from the pure, copy number unstable, uveal melanoma cell line Mel-202 (0% T cells). This cell line harbors a gain of the entire chromosome 7, encompassing the ΔB T-cell marker region.[21] Therefore, these mixtures are not correctly measurable following the

classic model, similar to the situation proposed in Figure 2C. Using the multiplex digital PCR experimental setup, five different mixtures were analyzed (Figure 5B). As expected, the higher the contribution of Mel-202 DNA, the larger the error in T-cell fraction according to the classic model. However, the adjusted model allowed us to correctly determine the fraction of T-cell DNA in all mixtures.

Application of the Adjusted Model in Copy Number Unstable Cutaneous Melanoma Biopsies

To practically apply and validate the utility of the classic and adjusted model, three cutaneous melanoma biopsies from independent patients were analyzed using the multiplex digital PCR experimental setup (Figure 6). These *BRAF* p.V600E mutant melanomas, two primary tumors (CM-1 and CM-2) and one metastatic lesion (CM-3), were selected on the basis of the presence of an additional copy number gain of *BRAF*. An overview of the available clinical-pathologic characteristics of the cases is presented in Supplemental Table S1. In line with the frequent co-occurrence of *BRAF* and *TRB* CNAs on chromosome 7q
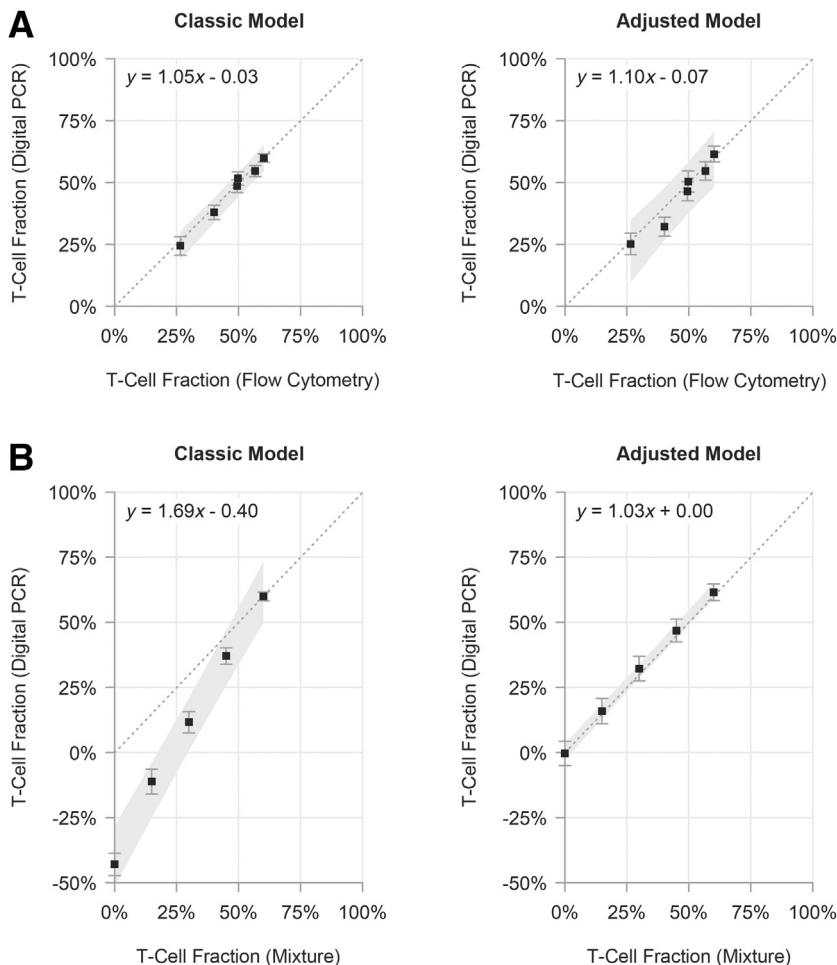
Figure 5 T-cell quantifications, according to classic and adjusted model, as determined by multiplex digital PCR in healthy peripheral blood mononuclear cells (PBMCs) and copy number unstable mixtures. The dotted lines represent perfect linear correlations ($y = x$), and the gray polygons denote the 95% prediction intervals. **A:** T-cell fractions, according to the classic and adjusted model (y axis), compared with the fractions measured by flow cytometry (x axis) in six healthy, copy number stable PBMC samples. Although accurate quantifications are obtained with both models, the variability of the measurements and individual 95% CIs are larger when following the adjusted model. **B:** T-cell fractions, according to the classic and adjusted model (y axis), compared with the expected fraction (x axis) in five DNA mixtures of a healthy, copy number stable PBMC sample with approximately 60% T cells and copy number unstable Mel-202 cell line with 0% T cells. The gain of chromosome 7 in Mel-202 causes an underestimation of the T-cell fraction following the classic model.
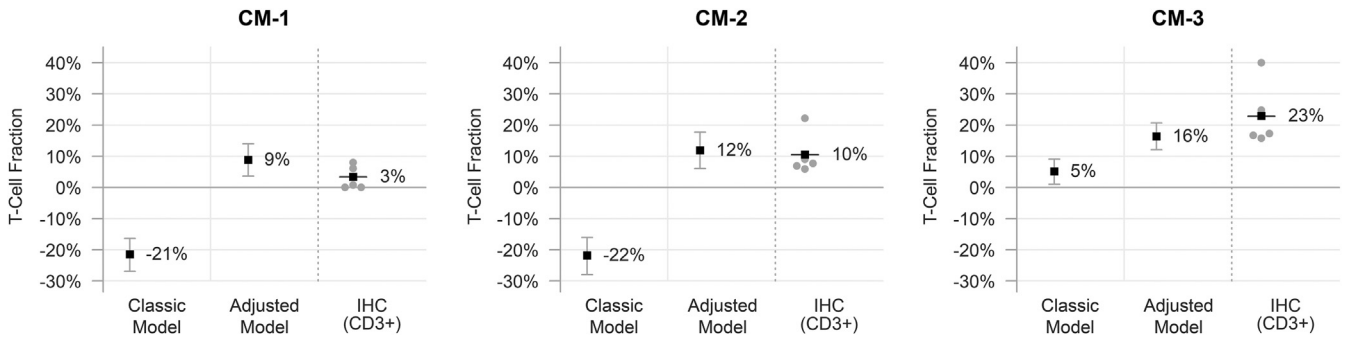
Figure 6 T-cell quantifications, according to the classic and adjusted model, and immunohistochemistry (IHC) in three cutaneous melanoma samples with a known copy number gain of *BRAF*. In all cases, this gain also involves the *TRB* locus and causes an underestimation of the T-cell fraction following the classic model, with even negative T-cell fraction in CM-1 and CM-2. The copy number–derived error is corrected using the adjusted model. The low to moderate levels of T cells are confirmed by taking the average (thick lines) of a CD3$^+$ immunohistochemical staining of five representative tumor areas (gray dots).

(Figure 1C), the ΔB T-cell marker region was also gained in these three specimens, resulting in an underestimation of the T-cell fraction following the classic model (Figure 6). This was most evident in CM-1 and CM-2, in which negative T-cell fractions of −21% and −22% were observed. In all cases, the T-cell fraction could be rescued by using the adjusted model with *TRBC2* as RC. The presence of the low to moderate levels of T cells was confirmed by immunohistochemistry (Figure 6 and Supplemental Figure S1).

Discussion

Genetic dissimilarities between cells can be effectively utilized to enumerate the presence of specific cell types in admixed DNA samples. This is particularly relevant in oncology, where newly acquired mutations distinguish tumor clones from genetically healthy cell populations. Detection of resistant or persistent tumor cells (ie, minimal residual disease) has considerable clinical relevance in many malignancies, both prognostically and therapeutically.[22] The same concept might be applied in the detection and quantification of healthy cell populations, such as immune cells. Similarly, the absolute presence of specific immune cell types has significant prognostic and therapeutic value in oncological care.[7,8] However, universal genetic markers for autologous, nonmalignant cell types are scarce, as most cells in the human body share a fully identical genome.

Previously, we identified two T-cell DNA markers (ie, ΔB and ΔD) that are biallelically deleted in nearly every T cell.[4] The origin of these markers lies in the genetic rearrangements of T-cell receptor genes during early T-cell development. As these processes do not take place in other cells, both markers are typically present on both alleles in non–T cells, making them generic and specific (Figure 2A). To accurately measure the presence of the T-cell DNA markers, a duplex digital PCR experimental setup was designed and technically validated.[4,5] More important,

however, somatic CNAs may also lead to the loss or gain of these markers, resulting in an underestimation or overestimation of the true T-cell abundance. The original classic model is therefore only valid in DNA samples that do not harbor a CNA involving the T-cell marker region. As most benign samples are copy number stable, the classic model can be safely applied in these samples. This was evidently illustrated in the validation experiments of our original report.[4]

However, the mathematical basis of the classic model may be distorted when a CNA affecting the T-cell marker region is present in admixed non–T cells, such as malignant cells (Figure 2B). When the T-cell marker region is lost in the sample of interest (eg, as a result of a chromosomal deletion in admixed cancer cells), the absence of the T-cell marker is not derived from T cells only, and the T-cell fraction will be too high. Vice versa, extra copies of the T-cell marker region may conceal the T-cell–derived loss of the marker and underestimate the true T-cell fraction (Figure 2C), or even result in a negative T-cell fraction. According to our pan-cancer analysis, such CNAs involving the ΔB and ΔD marker regions (ie, the *TRB* and *TRD* gene loci) occur in approximately 24% and approximately 17% of the tumors, respectively (Figure 1). Although these values may be surprisingly high, it is unlikely that the alterations are targeting the T-cell receptor genes specifically. These genes are not used in most malignancies and, as an example, the CNAs involving the ΔB marker region typically encompassed a much larger part of the chromosome. Still, these frequencies indicate that the original DNA-based T-cell quantification will fail in on average one of four (ΔB) or one of six (ΔD) of the cancer specimens, marking the need for a robust solution.

In this study, we introduced an extension of our original experimental setup, enabling the recognition and adjustment of copy number instability involving the T-cell marker region. This extended approach was evaluated *in silico* and validated *in vitro* using multiplex digital PCR.

The key elements of digital PCR (subsampling, random partitioning, end-point measurements, and consequent mathematical interpretation) can be effectively modeled *in silico*, providing important insights in the mathematical validity and precision of a given experimental setup.[12,23] This analysis demonstrated that under copy number stable conditions, the T-cell fraction is correctly estimated by using the adjusted model, but with slightly decreased precision than in the classic model (Figure 3A). These findings were confirmed by the analysis of healthy PBMC DNA samples using both the classic and adjusted model (Figure 5A). The reduced precision is likely to be explained by the insurmountable uncertainty of the extra measurement (ie, the RC) being taken into account in the calculations, whereas its value is not necessary for an accurate estimation of the T-cell fraction.

The additional value of the adjusted model is demonstrated when a CNA affects the T-cell marker region. Both our *in silico* and *in vitro* validation experiments showed that under such condition, the classic model fails to determine the true T-cell fraction, whereas the adjusted model recognizes and corrects the obtained error adequately (Figures 3B and 5B). Herein, the adjusted model was practically applied by a multiplex digital PCR experimental setup, which allowed us to analyze the T-cell marker, the RC, and the stable genomic reference concurrently within one experiment (Figure 4B). This setup required only half of the DNA and reagents compared with the duplex alternative, while giving the same results (Figure 4C). Consequently, the number of pipetting actions (and hence risk of errors) was reduced as well. This makes the multiplex approach an equally valid, but practically more efficient experimental setup.

As a proof of concept, the utility of our approach was evaluated in copy number unstable cutaneous melanoma DNA samples (Figure 6). Given the close proximity of the *TRB* gene to *BRAF*, an established oncogene in cutaneous melanoma and other cancers,[15,16] (focal) copy number increases targeting *BRAF* (found in up to 50% of the melanomas) typically also involve the ΔB T-cell marker region (Figure 1C). Using the multiplex digital PCR, these CNAs were detected, and the underestimated T-cell fractions were properly corrected, demonstrating that the adjusted model can be successfully applied to obtain T-cell fractions in copy number unstable tumor DNA specimens.

Consequently, our advanced multiplex digital PCR setup has several potential clinical and diagnostic applications in cancer. From a prognostic point of view, the magnitude of T-cell infiltration in tumors has been correlated to tumor growth and clinical outcome in various types of cancer.[7,8] For example, the quantified T-cell presence was found to be an independent prognostic factor associated with metastatic recurrence in resected primary cutaneous melanoma.[24] The extent of T-cell infiltration can also be used to predict response to neoadjuvant therapies.[25,26] Furthermore, (tumor-infiltrated) T cells are being increasingly used

therapeutically by the administration of drugs (eg, checkpoint inhibitors and bispecific antibodies).[27−30] The conventional methods for quantification of T-cell content in body fluids or solid tissues are flow cytometry and immunohistochemistry, which are based on using T-cell−specific antibodies.[31,32] However, these approaches require that specified T-cell epitopes are present and accessible in the sample of interest, which is highly dependent on the specimen's condition and method of preparation. Furthermore, tissue sampling biases and artifacts derived from unequal cell disaggregation or fixation may be present and influence the reliability of these methods. Consequently, when sample quantity and/or quality is low, the quantitative performance may be hampered and an alternative approach is needed. Our method shifts the focus from epitope expression to T-cell−specific DNA biomarkers. Advantageously, such DNA-based analysis can be performed more rapidly in samples of much lower quantity and quality, but may also reduce various forms of technical and biological measurement variability.[4,5,17,18] For example, when DNA is isolated from a larger proportion of the tumor, spatial differences in T-cell presence can be equaled out and the DNA-based quantification will be a better representation of the whole tumor. Moreover, but in contrast to conventional methods, digital PCR is less dependent on visual inspection and manual thresholding or interpretation.[33]

The validity our adjusted model is limited to samples where copy number stable T cells are mixed with (possibly) copy number unstable non−T cells. In (immature) T-cell lymphomas and leukemias, the maturation stage at onset of the malignancy, level of clonality, and genetic (in)stability may have consequences on the presence of the ΔB and ΔD T-cell markers.[34,35] As a result, our approach may underestimate or overestimate the presence of (malignant) T cells when analyzing T-cell proliferation. Additionally, in some malignancies, such as precursor B-acute lymphoblastic leukemias and acute myeloid leukemias, illegitimate rearrangements of the T-cell receptor genes have been reported.[10,11] The ΔB and ΔD T-cell markers may consequently be deleted in admixed leukemic B cells, giving an overestimation of the T-cell fraction in such samples. Taken together, particular care should be taken when analyzing samples from a lymphoproliferative origin.

Recently, high-throughput sequencing of the *TRB* gene was evaluated as a novel molecular method to quantify the fraction of T cells in melanoma and carcinoma.[24,36] This approach, commercially available as the immunoSEQ Assay (Adaptive Biotechnologies, Seattle, WA), is more complex than our method, but comparable in the sense that the T-cell abundance is estimated on the basis of comparing (un) rearranged T-cell receptor DNA with reference DNA. Recently and also similar to our work, a bioinformatical method was described to estimate T-cell fractions from whole-exome sequencing data based on the loss of *TRA/ TRD* DNA.[37] Advantageously, such measurements can be performed using existing sequencing data, whereas targeted

sequencing and our method require extra wet-laboratory experiments. However, it would be informative to analyze a large, diverse cohort of samples and compare our assay with these alternative approaches on accuracy, precision, applicability (including in DNA samples with high levels of fragmentation, such as those of formalin-fixed, paraffin-embedded origin), and performance under copy number instability.

Finally, it would be useful to extend our panel of assays with an RC for the ΔD T-cell marker, as CNAs affecting this marker region are also frequently observed (Figure 1B). A candidate RC may be found in the constant gene segment of the *TRA* gene, as *TRD* itself is located within *TRA* and consequently may be lost because of T-cell receptor rearrangements.[38]

In conclusion, our novel multiplex digital PCR setup offers a relatively simple, but accurate, T-cell quantification in copy number stable and unstable DNA samples. This approach has potential for clinical and diagnostic use as the quantitative performance is similar compared with current golden standards. Our DNA-based method, however, does not require T-cell—specific epitopes to be present and accessible, which means that the sample requirements are much lower.

Supplemental Data

Supplemental material for this article can be found at *http://doi.org/10.1016/j.jmoldx.2021.10.007*.

References

1. Davis MM, Bjorkman PJ: T-cell antigen receptor genes and T-cell recognition. Nature 1988, 334:395−402
2. van Dongen JJ, Langerak AW, Bruggemann M, Evans PA, Hummel M, Lavender FL, Delabesse E, Davi F, Schuuring E, Garcia-Sanz R, van Krieken JH, Droese J, Gonzalez D, Bastard C, White HE, Spaargaren M, Gonzalez M, Parreira A, Smith JL, Morgan GJ, Kneba M, Macintyre EA: Design and standardization of PCR primers and protocols for detection of clonal immunoglobulin and T-cell receptor gene recombinations in suspect lymphoproliferations: report of the BIOMED-2 Concerted Action BMH4-CT98-3936. Leukemia 2003, 17:2257−2317
3. Starr TK, Jameson SC, Hogquist KA: Positive and negative selection of T cells. Annu Rev Immunol 2003, 21:139−176
4. Zoutman WH, Nell RJ, Versluis M, van Steenderen D, Lalai RN, Out-Luiting JJ, de Lange MJ, Vermeer MH, Langerak AW, van der Velden PA: Accurate quantification of T cells by measuring loss of germline T-cell receptor loci with generic single duplex droplet digital PCR assays. J Mol Diagn 2017, 19:236−243
5. Zoutman WH, Nell RJ, van der Velden PA: Usage of droplet digital PCR (ddPCR) assays for T cell quantification in cancer. Methods Mol Biol 2019, 1884:1−14
6. Taylor AM, Shih J, Ha G, Gao GF, Zhang X, Berger AC, Schumacher SE, Wang C, Hu H, Liu J, Lazar AJ; Cancer Genome Atlas Research Network, Cherniack AD, Beroukhim R, Meyerson M: Genomic and functional approaches to understanding cancer aneuploidy. Cancer Cell 2018, 33:676−689.e3
7. Talmadge JE: Immune cell infiltration of primary and metastatic lesions: mechanisms and clinical impact. Semin Cancer Biol 2011, 21: 131−138
8. Fridman WH, Galon J, Pages F, Tartour E, Sautes-Fridman C, Kroemer G: Prognostic and predictive impact of intra- and peritumoral immune infiltrates. Cancer Res 2011, 71:5601−5605
9. Cancer Genome Atlas Research Network, Weinstein JN, Collisson EA, Mills GB, Shaw KR, Ozenberger BA, Ellrott K, Shmulevich I, Sander C, Stuart JM: The Cancer Genome Atlas Pan-Cancer analysis project. Nat Genet 2013, 45:1113−1120
10. Szczepanski T, Beishuizen A, Pongers-Willemse MJ, Hahlen K, Van Wering ER, Wijkhuijs AJM, Tibbe GJM, De Bruijn MAC, Van Dongen JJM: Cross-lineage T cell receptor gene rearrangements occur in more than ninety percent of childhood precursor-B acute lymphoblastic leukemias: alternative PCR targets for detection of minimal residual disease. Leukemia 1999, 13:196−205
11. Przybylski G, Oettle H, Ludwig W, Siegert W, Schmidt C: Molecular characterization of illegitimate TCRδ gene rearrangements in acute myeloid leukaemia. Br J Haematol 1994, 87:301−307
12. Dube S, Qin J, Ramakrishnan R: Mathematical analysis of copy number variation in a DNA sample using digital PCR on a nano-fluidic device. PLoS One 2008, 3:e2876
13. Katz D, Baptista J, Azen S, Pike M: Obtaining confidence intervals for the risk ratio in cohort studies. Biometrics 1978, 34:469−474
14. Verbik DJ, Murray TG, Tran JM, Ksander BR: Melanomas that develop within the eye inhibit lymphocyte proliferation. Int J Cancer 1997, 73:470−478
15. Corcoran RB, Dias-Santagata D, Bergethon K, Iafrate AJ, Settleman J, Engelman JA: BRAF gene amplification can promote acquired resistance to MEK inhibitors in cancer cells harboring the BRAF V600E mutation. Sci Signal 2010, 3:ra84
16. Shain AH, Joseph NM, Yu R, Benhamida J, Liu S, Prow T, Ruben B, North J, Pincus L, Yeh I, Judson R, Bastian BC: Genomic and transcriptomic analysis reveals incremental disruption of key signaling pathways during melanoma evolution. Cancer Cell 2018, 34:45−55.e44
17. de Lange MJ, Nell RJ, Lalai RN, Versluis M, Jordanova ES, Luyten GPM, Jager MJ, van der Burg SH, Zoutman WH, van Hall T, van der Velden PA: Digital PCR-based T-cell quantification-assisted deconvolution of the microenvironment reveals that activated macrophages drive tumor inflammation in uveal melanoma. Mol Cancer Res 2018, 16:1902−1911
18. Yurick D, Khoury G, Clemens B, Loh L, Pham H, Kedzierska K, Einsiedel L, Purcell D: Multiplex droplet digital PCR assay for quantification of human T-cell leukemia virus type 1 subtype c DNA proviral load and T cells from blood and respiratory exudates sampled in a remote setting. J Clin Microbiol 2019, 57:e01063-18
19. Zhong Q, Bhattacharya S, Kotsopoulos S, Olson J, Taly V, Griffiths AD, Link DR, Larson JW: Multiplex digital PCR: breaking the one target per color barrier of quantitative PCR. Lab Chip 2011, 11:2167−2174
20. Whale AS, Huggett JF, Tzonev S: Fundamentals of multiplexing with digital PCR. Biomol Detect Quantif 2016, 10:15−23
21. Nareyeck G, Zeschnigk M, Prescher G, Lohmann DR, Anastassiou G: Establishment and characterization of two uveal melanoma cell lines derived from tumors with loss of one chromosome 3. Exp Eye Res 2006, 83:858−864
22. Cescon DW, Bratman SV, Chan SM, Siu LL: Circulating tumor DNA and liquid biopsy in oncology. Nat Cancer 2020, 1:276−290
23. Nell RJ, van Steenderen D, Menger NV, Weitering TJ, Versluis M, van der Velden PA: Quantification of DNA methylation independent of sodium bisulfite conversion using methylation-sensitive restriction enzymes and digital PCR. Hum Mutat 2020, 41:2205−2216
24. Pruessmann W, Rytlewski J, Wilmott J, Mihm MC Jr, Attrill GH, Dyring-Andersen B, Fields P, Zhan Q, Colebatch AJ, Ferguson PM, Thompson JF, Kallenbach K, Yusko E, Clark RA, Robins H, Scolyer RA, Kupper TS: Molecular analysis of primary melanoma T

cells identifies patients at risk for metastatic recurrence. Nat Cancer 2020, 1:197−209

25. Castaneda CA, Mittendorf E, Casavilca S, Wu Y, Castillo M, Arboleda P, Nunez T, Guerra H, Barrionuevo C, Dolores-Cerna K, Belmar-Lopez C, Abugattas J, Calderon G, De La Cruz M, Cotrina M, Dunstan J, Gomez HL, Vidaurre T: Tumor infiltrating lymphocytes in triple negative breast cancer receiving neoadjuvant chemotherapy. World J Clin Oncol 2016, 7:387−394

26. Schatton T, Scolyer RA, Thompson JF, Mihm MC Jr: Tumor-infiltrating lymphocytes and their significance in melanoma prognosis. Methods Mol Biol 2014, 1102:287−324

27. Henricks LM, Schellens JH, Huitema AD, Beijnen JH: The use of combinations of monoclonal antibodies in clinical oncology. Cancer Treat Rev 2015, 41:859−867

28. Whiteside TL, Demaria S, Rodriguez-Ruiz ME, Zarour HM, Melero I: Emerging opportunities and challenges in cancer immunotherapy. Clin Cancer Res 2016, 22:1845−1855

29. Damato BE, Dukes J, Goodall H, Carvajal RD: Tebentafusp: T cell redirection for the treatment of metastatic uveal melanoma. Cancers (Basel) 2019, 11:971

30. Nathan P, Hassel JC, Rutkowski P, Baurain JF, Butler MO, Schlaak M, Sullivan RJ, Ochsenreither S, Dummer R, Kirkwood JM, Joshua AM, Sacco JJ, Shoushtari AN, Orloff M, Piulats JM, Milhem M, Salama AKS, Curti B, Demidov L, Gastaud L, Mauch C, Yushak M, Carvajal RD, Hamid O, Abdullah SE, Holland C, Goodall H, Piperno-Neumann S; IMCgp100-202 Investigators: Overall survival benefit with tebentafusp in metastatic uveal melanoma. N Engl J Med 2021, 385:1196−1206

31. Wood B, Jevremovic D, Bene MC, Yan M, Jacobs P, Litwin V: Validation of cell-based fluorescence assays: practice guidelines from the ICSH and ICCS - part V - assay performance criteria. Cytometry B Clin Cytom 2013, 84:315−323

32. Walker RA: Quantification of immunohistochemistry–issues concerning methods, utility and semiquantitative assessment I. Histopathology 2006, 49:406−410

33. Vogelstein B, Kinzler KW: Digital PCR. Proc Natl Acad Sci U S A 1999, 96:9236−9241

34. Zuurbier L, Gutierrez A, Mullighan CG, Cante-Barrett K, Gevaert AO, de Rooi J, Li Y, Smits WK, Buijs-Gladdines JG, Sonneveld E, Look AT, Horstmann M, Pieters R, Meijerink JP: Immature MEF2C-dysregulated T-cell leukemia patients have an early T-cell precursor acute lymphoblastic leukemia gene signature and typically have non-rearranged T-cell receptors. Haematologica 2014, 99:94−102

35. Villarese P, Lours C, Trinquand A, Le Noir S, Belhocine M, Lhermitte L, Cieslak A, Tesio M, Petit A, LeLorch M, Spicuglia S, Ifrah N, Dombret H, Langerak AW, Boissel N, Macintyre E, Asnafi V: TCRalpha rearrangements identify a subgroup of NKL-deregulated adult T-ALLs associated with favorable outcome. Leukemia 2018, 32:61−71

36. Van Abel KM, Routman DM, Moore EJ, Ma DJ, Yin LX, Fields PA, Schofield M, Bartemes KR, Chatzopoulos K, Price DL, Janus JR, Kasperbauer JL, Price KA, Chintakuntlawar AV, Neben-Wittich MA, Foote RL, Garcia JJ: T cell fraction impacts oncologic outcomes in human papillomavirus associated oropharyngeal squamous cell carcinoma. Oral Oncol 2020, 111:104894

37. Bentham R, Litchfield K, Watkins TBK, Lim EL, Rosenthal R, Martinez-Ruiz C, Hiley CT, Bakir MA, Salgado R, Moore DA, Jamal-Hanjani M; TRACERx Consortium, Swanton C, McGranahan N: Using DNA sequencing data to quantify T cell fraction and therapy response. Nature 2021, 597:555−560

38. Dik WA, Pike-Overzet K, Weerkamp F, de Ridder D, de Haas EF, Baert MR, van der Spek P, Koster EE, Reinders MJ, van Dongen JJ, Langerak AW, Staal FJ: New insights on human T cell development by quantitative T cell receptor gene rearrangement studies and gene expression profiling. J Exp Med 2005, 201:1715−1723